PHYSICAL REVIEW C **72**, 061301(R) (2005)

Search for excited states in ^{7}He with the (d, p) reaction

A. H. Wuosmaa,[1] K. E. Rehm,[2] J. P. Greene,[2] D. J. Henderson,[2] R. V. F. Janssens,[2] C. L. Jiang,[2] L. Jisonna,[3] E. F. Moore,[2] R. C. Pardo,[2] M. Paul,[4] D. Peterson,[2] Steven C. Pieper,[2] G. Savard,[2] J. P. Schiffer,[2] R. E. Segel,[3] S. Sinha,[2] X. Tang,[2] and R. B. Wiringa[2]

[1]*Physics Department, Western Michigan University, Kalamazoo, Michigan 49008-5252, USA*
[2]*Physics Division, Argonne National Laboratory, 9700 S. Cass Ave, Argonne Illinois 60439, USA*
[3]*Physics Department, Northwestern University, Evanston, Illinois 60208, USA*
[4]*Hebrew University, Jerusalem, Israel 91904*

(Received 10 March 2005; published 20 December 2005)

We have studied the properties of low-lying levels in ^{7}He using the ^{2}H(^{6}He, p)^{7}He reaction at 11.5 MeV/u. This reaction probes the $^6\mathrm{He}_{\mathrm{g.s.}} + n$ character of states in ^{7}He. The ground state was populated with a spectroscopic factor comparable to that obtained from *ab initio* calculations, supporting the tentative spin-parity assignment of $3/2^-$ in the literature. In addition to the ground state, a broad structure is observed between $E_X = 2$–3 MeV, the excitation-energy range expected for the $1/2^-$ state in ^{7}He. No evidence was found for a lower-lying, first-excited state reported recently.

DOI: 10.1103/PhysRevC.72.061301 PACS number(s): 21.10.Jx, 21.10.Hw, 25.60.Je, 27.20.+n

One of the few light nuclei whose structure remains uncertain is ^{7}He, which has no particle-bound states. Its ground state, first identified by Stokes and Young [1,2], lies 0.44 MeV above the $^6\mathrm{He}_{\mathrm{g.s.}} + n$ threshold, with a width of 150 $\pm$ 20 keV and a suggested spin-parity value of $3/2^-$ [3]. Beyond the ground state, the information in the literature is contradictory. Considerable theoretical and experimental effort has been devoted recently to understanding the properties of the excited levels in this system. The (d, p) reaction, used in this experiment, probes the simple $^6\mathrm{He}_{\mathrm{g.s.}} + n$ character of the configurations in ^{7}He.

Calculations carried out using the conventional Cohen-Kurath shell model [4] (CK), a $(0 + 2)\hbar\omega$ shell model [5] (WHG), a large-basis no-core shell model [6] (NCSM), and the Green's function Monte-Carlo [7] (GFMC) approach, all predict a sequence of negative parity levels starting with a $3/2^-$ ground state, followed by a $1/2^-$ state at 2–3 MeV excitation, as shown in Table I. At higher excitation energy, the theoretical calculations also predict a $5/2^-$ level, as well as a second $3/2^-$ state. Table I also gives spectroscopic factors obtained from the CK wave functions and from variational Monte Carlo (VMC) wave functions that are used to initiate the GFMC energy calculations. These spectroscopic factors indicate that the ground and first-excited states have large components consisting of a $p_{3/2}$ and $p_{1/2}$ neutron coupled to the $^6\mathrm{He}_{\mathrm{g.s.}}$ core, respectively. In contrast, the two higher excited levels each have very little overlap with neutrons coupled to $^6\mathrm{He}_{\mathrm{g.s.}}$; all states have significant coupling to the 1.797 MeV $^6\mathrm{He}(2^+)$ state. In other neutron-rich light nuclei (e.g., ^{9}Be and ^{11}Be), even-parity $1/2^+$ states occur at low excitation energy, and most of the theoretical calculations do not address these. It is, however, unlikely that such a state would be sufficiently confined to produce an observable resonance in ^{7}He. The resonating group model (RGM) has also been applied to this system to study both energies and widths [8]. The $3/2^-$ ground state is predicted to have a width in good agreement with the measured value. The first-excited state is a $J^\pi = 1/2^-$ resonance, but its position and width are less certain, with an excitation energy, E_X, between 2 and 3 MeV, and a width, Γ, between 1 and 3 MeV.

Contradictions remain, however, among the available experimental results. Bohlen *et al*. studied the heavy-ion transfer reaction ^{9}Be(^{15}N,^{17}F)^{7}He and identified a broad state at $E_X =$ 2.9 MeV, with a width of approximately 2 MeV [9]. A level with similar properties was also identified in the p(^{8}He, d)^{7}He reaction [10]. In the latter work this resonance was reported to decay predominantly via $^4\mathrm{He} + 3n$, i.e., through the 2^+ excitation in ^{6}He, and a tentative spin assignment of $J^\pi = 5/2^-$ was proposed on the basis of this observed decay mode. Other than this broad resonance and the ground state, however, no other prominent structures were observed, leaving open the question of the position of the expected $1/2^-$ first excited state. The same reaction to the ^{7}He ground state has recently been studied by Skaza *et al*., who reported a (p, d) neutron pickup spectroscopic factor of 3.3 [11]. A study by Meister *et al*. [12] of ^{8}He breakup on a ^{12}C target at higher energies reported evidence for a new, low-lying state in ^{7}He, inferred from an extended tail in the $^6\mathrm{He} + n$ momentum correlation spectrum. This level was attributed to a $1/2^-$ state at $E_X =$ 600 keV with $\Gamma = 750$ keV. No such level has been observed in either the heavy-ion transfer or the neutron-pickup reaction. A very recent report [13] of the ^{2}H(^{7}Li, ^{2}He)^{7}He reaction shows some evidence for a broad level near 2.9 MeV, but none for a lower-lying first-excited state, such as that reported in Ref. [12]. Finally, work by Rogachev *et al*. [14] and Boutachkov *et al*. [15] studied analog states at high excitation energy in ^{7}Li via $^6\mathrm{He} + p$ elastic and inelastic scattering. No evidence for a narrow low-lying $1/2^-$ resonance was reported, although the data do allow for a broader state above an excitation energy of 2.2 MeV. The reported low-lying first-excited state is difficult to reconcile with the other data and with theoretical calculations, although a recent result obtained with the recoil corrected continuum shell model (RCCSM) may be consistent with such a level [16].

TABLE I. Theoretical excitation energies and spectroscopic factors: E_X in MeV for states in ^{7}He are from Refs. [4–7]; spectroscopic factors are S_0 for $^6\mathrm{He}(0^+) + n \rightarrow {}^7\mathrm{He}$ and S_2 for $^6\mathrm{He}(2^+) + n \rightarrow {}^7\mathrm{He}$.

J^π	E_X				S_0		S_2	
	CK	WHG	NCSM	GFMC	CK	VMC	CK	VMC
$3/2^-$	0.00	0.0	0.0	0.0	0.59	0.53	1.21	1.76
$1/2^-$	2.56	2.5	2.3	2.9(3)	0.69	0.87	0.60	0.34
$5/2^-$	3.64	3.4	3.7	3.3(2)	0.00	0.00	1.36	1.20
$3/2^-$	3.88	4.6	4.4	3.8(2)	0.06	0.06	1.38	1.11

Most of these studies used complex reactions that are not easily related to calculable nuclear structure properties. The interpretation of (d, p) reactions is, however, straightforward; a ^{2}H(^{6}He, p)^{7}He neutron stripping reaction to narrow final states, at incident energies above 4 and below about 10 MeV/nucleon, should selectively populate those states in ^{7}He that have strong $^6\mathrm{He}_{\mathrm{g.s.}} + n$ character, and thus a $1/2^-$ level should be populated strongly and unambiguously. Other, higher excited states with $J^\pi = 5/2^-$ or $3/2^-$ are expected to be populated only very weakly, if at all. One report about the ^{2}H(^{6}He, p)^{7}He reaction at a bombarding energy of 30 MeV/nucleon has been presented [17]. No conclusions were given about the first-excited state, however, other than that a narrow $1/2^-$ level was not observed.

To address some of these issues, we have studied the ^{2}H(^{6}He, p)^{7}He reaction at a bombarding energy of 11.5 MeV/nucleon. The energy was chosen as a compromise between the optimum energy for interpreting neutron stripping reactions and conditions that make the detection of the protons feasible in the crucial backward laboratory angular range.

The measurement was carried out with a ^{6}He beam produced at the "in-flight" RIB production facility at the ATLAS accelerator of Argonne National Laboratory [18]. An 81-MeV ^{7}Li beam with an intensity of 55 pnA bombarded a LN_2-cooled cell filled to a pressure of 1250 mbar with D_2 gas, and the secondary ^{6}He beam was produced by the ^{2}H(^{7}Li, ^{6}He)^{3}He reaction. The ^{6}He projectiles were collected with a 6T superconducting solenoid and were separated from the primary ^{7}Li beam by a bending magnet and slit system. There was no observable contamination from the primary ^{7}Li beam; a $<10\%$ contamination of low-energy protons did not interfere with the measurement. The resulting ^{6}He energy was 69 MeV, with an intensity of about 10^4 particles/s.

The ^{6}He beam bombarded a $(CD_2)_n$ target, 540 μg/cm^2 thick. The reaction products were detected in an array of silicon detectors. Protons were detected, and their energies and angles were measured, with three segmented annular silicon detectors in the angular range $109^\circ < \theta_{\mathrm{lab}} < 159^\circ$, corresponding to forward proton angles in the center-of-mass system. The recoiling ^{4,6}He particles were identified in coincidence with protons in an array of silicon ΔE-E telescopes covering laboratory angles between 1.3° and 7.3° and nearly the entire 2π azimuthal range. The experimental setup was identical to that described in Ref. [19].

The intensity of the incident ^{6}He beam was monitored in two ways; downstream of the ΔE-E array, a gold target was used to scatter the beam into a second ΔE-E telescope, where the intensity was continuously measured. Second, a downscaled fraction of singles events from the ΔE-E array was recorded to monitor the ^{6}He particles elastically scattered from ^{12}C nuclei in the $(CD_2)_n$ target. The two normalization methods agreed to within 10%.

To understand the efficiency, resolution and threshold properties of the proton detectors, the primary ^{7}Li beam was transported to the target, after being degraded in the secondary beam production cell. A ^{2}H(^{7}Li, p)^{8}Li ($Q_g = -0.192$ MeV) Q-value spectrum is shown in Fig. 1(a) for events with protons in coincidence with ^{7,8}Li ions. The three lowest states in ^{8}Li are apparent. The excitation-energy resolution of approximately 350 keV full width at half maximum (FWHM) is dominated by a combination of the detector energy resolution and the size of the proton-detector segments, (approximately 1°). The Q-value dependence of the total detection efficiency was obtained from Monte Carlo simulations of the experimental setup, where the low-energy response of the proton detectors was determined from the data from the ^{2}H(^{7}Li, p)^{8}Li reaction. The efficiency

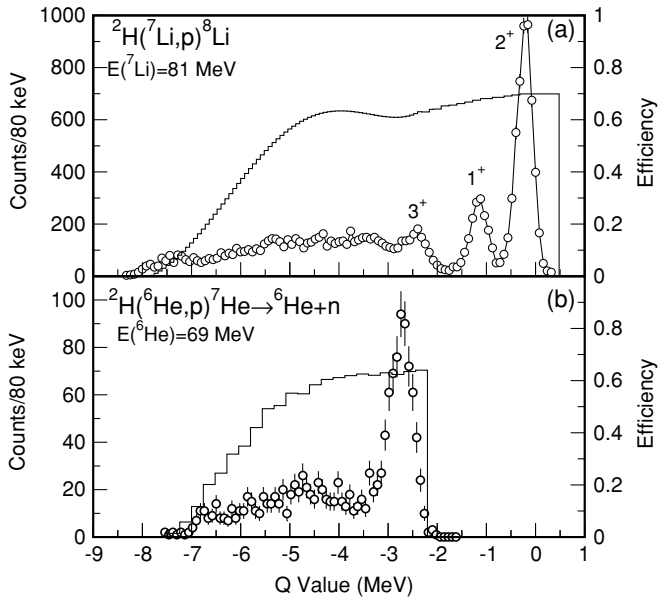

FIG. 1. (a) Q-value spectrum for the ^{2}H(^{7}Li, p)^{8}Li reaction from p-^{7,8}Li coincidence events. (b) Q-value spectrum for the ^{2}H(^{6}He, p)^{7}He reaction from p-^{6}He coincidence events. In both cases the data are taken over the entire angular range covered by the proton detectors ($\theta_{\mathrm{lab}} = 109^\circ$ to 159°). The histograms represent the Q-value dependence of the total detection efficiency.

for ^{2}H(^{7}Li, p)^{8}Li appears as the thin histogram in Fig. 1(a). The inflection point near $Q = -3$ MeV arises from the opening of the p-^{7}Li-n final state at $Q = -2.22$ MeV. The total numbers of incident ^{6}He and ^{7}Li particles were $4.4 \pm 0.4 \times 10^9$ and $1.6 \pm 0.2 \times 10^{10}$, respectively.

The ^{2}H(^{6}He, p)^{7}He ($Q_g = -2.669$ MeV) Q-value spectrum derived from all ^{6}He-p coincidences is presented in Fig. 1(b). Because of the lower bombarding energy and more negative ground-state Q value for the reaction, the ^{2}H(^{6}He, p)^{7}He spectrum extends to smaller excitation energies than that for ^{2}H(^{7}Li, p)^{8}Li. The ground state is clearly populated, and the measured ground-state Q value is consistent with the value in the literature [3]. At higher excitation energy, a broad distribution of counts is observed that peaks near $Q = -5$ MeV. The histogram in Fig. 1(b) represents the Q-value dependence of the ^{6}He-p coincidence efficiency from Monte Carlo simulations of the p-^{6}He-n final state as described above. The falloff at high excitation arises from a combination of kinematic coincidence efficiency and low-energy thresholds of the proton detectors.

The data for ^{2}H(^{7}Li, p)^{8}Li and ^{2}H(^{6}He, p)^{7}He, corrected for detection efficiency, are presented in Fig. 2(a) and 2(b), respectively. To reproduce the shape of the experimental spectrum for ^{7}He, peak shapes were constructed using the ground-state width of 150 keV and another broad resonance with variable parameters. An empirical "background" was also included to approximate a continuum produced by $d \rightarrow n + p$ breakup. This "background" was derived from the shape of the ^{2}H(^{7}Li, p)^{8}Li spectrum above the one-neutron decay threshold in ^{8}Li as shown by the dashed curve in Fig. 2(a) and was assumed for fitting purposes to be incoherent with the resonant contribution, an assumption that is used for want of better alternatives. The resonance shapes were generated using the R-matrix formalism, assuming $\ell = 1$ neutrons, and a range of excitation energies and reduced widths. These shapes were then folded with the Q-value dependence of the (d, p) reaction cross section calculated with the finite-range distorted wave born approximation (DWBA) program PTOLEMY [20]. This folding has the effect of shifting the R-matrix peak energy to lower values for broad states above $E_X = 2$ MeV [see Fig. 3(a)]. All peaks were convoluted with the experimental Q-value resolution.

For each R-matrix shape at a given value of E_X and Γ, the total spectrum was constructed by varying the relative contributions of the ground and excited states and empirical background. The experimental data are most consistent with a calculated resonance shape that has a peak at $E_X = 2.6$ MeV and $\Gamma_{\mathrm{FWHM}} = 2.0$ MeV, with the full fit given as the thick line in Fig. 2(b). Figure 3(a) shows the final resonance shapes, and the individual contributions to the total fit are given as histograms in Fig. 2(b). The total numbers of efficiency-corrected counts for the ground state and broad resonance determined from this fitting procedure were 870 ± 50 and 570 ± 100, respectively. The background contribution within the region corresponding to the broad resonance contributed 700 ± 100 counts. To assess the significance of the results for the presence of a broad state, in Fig. 3(b) we show the dependence of χ^2 on the number of counts in the broad resonance, subject to the constraint that the total resonance + background

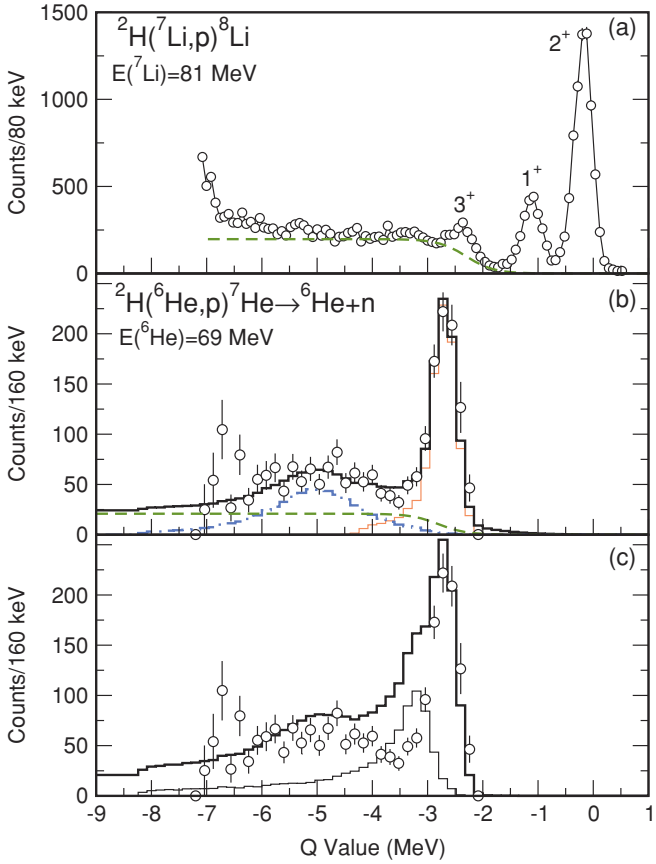

FIG. 2. (Color online) (a) Q-value spectrum for the ^{2}H(^{7}Li, p)^{8}Li reaction from p-^{7,8}Li coincidence events corrected for detection efficiency. The dashed line represents the empirical continuum described in the text. (b) Q-value spectrum for the ^{2}H(^{6}He, p)^{7}He reaction from p-^{6}He coincidence events corrected for detection efficiency. The solid line corresponds to the total fit to the spectrum described in the text. The thin, dot-dashed, and dashed lines represent the ground-state, broad resonance, and continuum contributions to the total fit as described in the text. (c) ^{2}H(^{6}He, p)^{7}He Q-value spectrum with fit (thick histogram) that includes the contributions of a low-lying first-excited state. The thin histogram illustrates the the expected contribution from the 600-keV state alone.

counts equal the experimental yield. The curve displays a distinct minimum, and the curvature is used to determine the uncertainties quoted above.

A resonance with the properties of the low-lying level reported in the ^{8}He breakup work of Ref. [12], namely $E_X = 600$ keV and $\Gamma_{\mathrm{FWHM}} = 750$ keV, is also shown as the dot-dashed curve in Fig. 3(a). The peak of such a resonance would appear almost exactly in the valley between the ground state and the broad resonance in the present ^{2}H(^{6}He, p)^{7}He data of Fig. 2(b). A state with this neutron width (proportional to the spectroscopic factor) and the expected spectroscopic factor for the $1/2^-$ state should appear with a large cross section.

Fits including not only the ground state, broad state, and continuum but also varying contributions of an assumed 600-keV state were made. The best fit using the above values for the ground and broad states resulted in efficiency-corrected

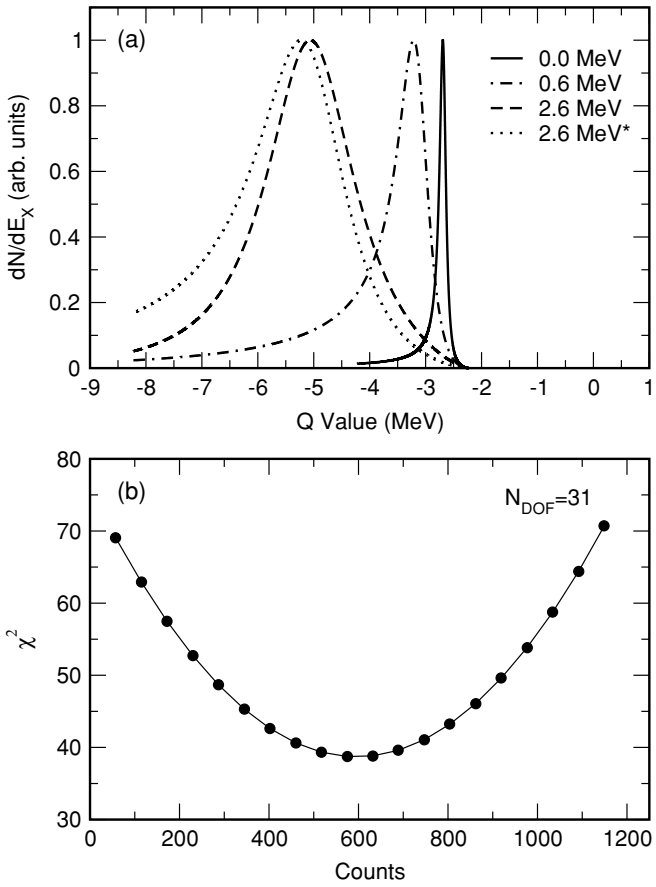

FIG. 3. (a) Line shapes of states included in the analysis of the ^{2}H(^{6}He, p)^{7}He data. The ground state, 600-keV state, and 2.6-MeV state are given by the thin solid, dot-dashed, and dashed lines, respectively. The profile of the broad state before including the effects of DWBA folding is given by the dotted line. (b) Plot of χ^2 versus yield for the 2.6 MeV resonance.

values identical to those quoted above and 0 ± 20 for an assumed 600-keV state. The DWBA calculations described below would result in a total cross section for a $1/2^-$ state at 600 keV that is approximately equal to 0.96 times that of the ground state, or 840 counts, using the calculated spectroscopic factors from Table I with the ground-state value renormalized as discussed below. In comparison to the VMC spectroscopic factor in Table I, the corresponding 3σ upper limit on the $^6\mathrm{He}_{\mathrm{g.s.}} + n$ spectroscopic factor for such a state is 0.07. The histogram in Fig. 2(c) shows the simulated spectrum obtained including the low-lying $1/2^-$ state populated with the calculated VMC spectroscopic factor (thick line) and the profile of the 600 keV state alone (thin line). These results indicate that any structure near a 600-keV excitation energy in ^{7}He cannot correspond to a $1/2^-$ state with the theoretically anticipated spectroscopic factors of order 0.7 or larger.

The angular distributions for both the ground state and the 2.6 MeV resonance are presented in Fig. 4. The cross sections were obtained from yields determined from the total integrals of the peak shapes, with normalization obtained from the fitting procedure described above for each angle bin. Also shown for comparison is the total experimental cross section without

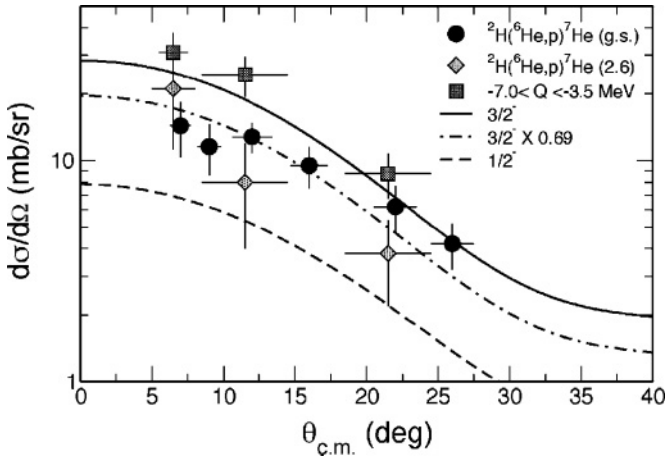

FIG. 4. Angular distributions for ^{2}H(^{6}He, p)^{7}He. The circles correspond to the ground state, and the diamonds and squares to the possible broad excited state, with and without background subtraction, respectively. The curves represent DWBA calculations described in the text.

continuum subtraction for $-7.0 < Q < -3.5$ MeV (squares). In all cases the horizontal error bars represent the angle range covered for each data point. The angular distributions for both transitions are forward peaked. For the possible excited state, limited statistics and excitation-energy range may result in a less reliable separation of continuum and resonance for the most forward-angle point, and the uncertainties are larger than those for the total spectrum discussed above.

The curves in Fig. 4 represent angular distributions calculated with PTOLEMY. The ground-state $^6\mathrm{He}_{\mathrm{g.s.}} + n(p_{3/2})$ and first-excited-state $^6\mathrm{He}_{\mathrm{g.s.}} + n(p_{1/2})$ spectroscopic factors of 0.53 and 0.87, respectively, are from a VMC calculation of the type described in Ref. [7]. The excited-state yields assume a resonance profile as described above and include the effects of the Q-value dependence of the calculated (d, p) cross section. The form factors were calculated by fixing the neutron separation energy to 0.2 MeV, as described in Ref. [19]. The optical potential parameters are those of set 1 also from Ref. [19]. These parameters were fit to elastic scattering of protons and deuterons from the stable p-shell nuclei, however, and are not necessarily appropriate for ^{6}He which is more diffuse.

The calculated ground-state cross section is in fair agreement with the data, though somewhat high at forward angles. Better agreement is achieved by renormalizing the curve by a factor of 0.69 (dot-dashed line in Fig. 4); such a renormalization corresponds to an experimental neutron spectroscopic factor of 0.37 ± 0.07, where the uncertainty is predominantly from the statistical uncertainties in the data. For the broad state, the cross section from the fitting procedure described above is consistently higher than the prediction for a $1/2^-$ state. The higher yield here may reflect additional effects that are not included in the reaction formalism used here for the extraction of spectroscopic factors for broad states.

A ^{7}He resonance at $E_X = 2.6$ MeV can decay to both the 0^+ and 2^+ states of ^{6}He and Table I indicates that the $1/2^-$ level is predicted to have significant spectroscopic factors for decay to

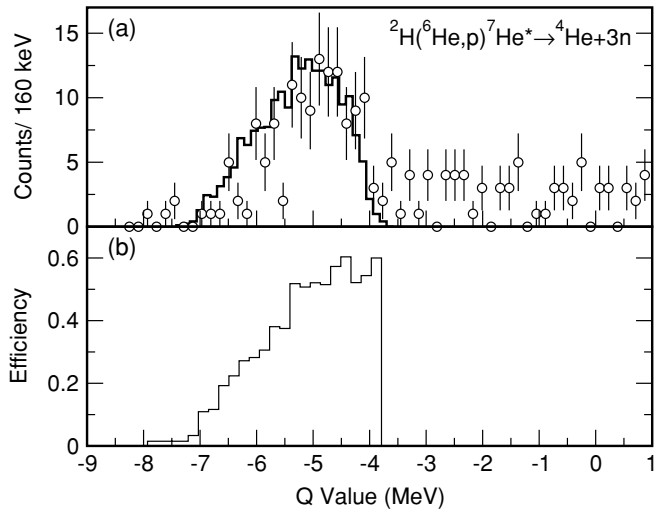

FIG. 5. (a) Q-value spectrum for ^{2}H(^{6}He, p)^{7}He* for ^{7}He$^* \rightarrow$ ^{4}He $+ 3n$ decays from ^{4}He $+ p$ coincidences, not corrected for efficiency. The histogram represents the distribution of counts expected for the state at $E_X = 2.6$ MeV shown in Fig. 3(a), and is presented for purposes of illustration only. (b) ^{4}He $+ p$ detection efficiency.

^{6}He(2^+). The ^{7}He$^* \rightarrow ^4$He $+ 3n$ channel that is the signature of decay through the ^{6}He(2^+) excitation, was studied by constructing a Q-value spectrum for protons in coincidence with α particles identified in the forward ΔE-E array. The resulting spectrum appears in Fig. 5(a). Although statistics are low, there is an enhancement of counts beginning at $E_X \approx 1.3$ MeV and extending to higher excitation energies. A Monte Carlo simulation of the five-body $p+^4$He $+ 3n$ final state, assuming decay through the first-excited state in ^{6}He, produces the efficiency curve shown in Fig. 5(b). The thick histogram in Fig. 5(a) is shown solely to illustrate the expected location of the yield from the ^{7}He$^* \rightarrow ^4$ He $+ 3n$ decay.

The experimental background in Fig. 5(a) for $Q > -4$ MeV likely arises from reactions of ^{6}He with ^{12}C nuclei in the CD_2 target. A short measurement with a pure ^{12}C target indicated that such reactions produce events uniformly distributed throughout the observable region for such Q values. The subtraction of a constant background leaves 90 ± 18 counts for ^{4}He-p coincidences from ^{7}He*. Assuming the same "peak"-to-total ratio deduced from the p-^{6}He coincidence data for the broad resonance (0.45), we would then attribute 40 ± 7 of those counts to a possible ^{7}He resonance. With efficiency correction, this value translates into a ^{6}He(2^+) branching ratio of 0.2 ± 0.1; however, given the uncertainties, this result should be treated as a rough estimate. The R-matrix calculations described above for the $1/2^-$ VMC spectroscopic factors given in Table I predict a branching ratio of 0.1.

If the yield above $E_X = 1.0$ MeV can be partially attributed to a first-excited state of ^{7}He, its position and width are generally in accord with the results of recent theoretical calculations. The width and the small decay branch to the first-excited state of ^{6}He are consistent with expectations for a $1/2^-$ level with strong ^{6}He$_{\text{g.s.}} + n$ single-particle character, although the cross section is somewhat larger than the expectations for a single $1/2^-$ state. The observed excitation energy for the maximum is slightly lower than the broad resonance observed in the heavy-ion transfer, and neutron pickup measurements, perhaps suggesting that different states are populated in the different reactions, or that a possible coherence between breakup and transfer could yield a different shape.

In conclusion, we have studied the ^{2}H(^{6}He, p)^{7}He reaction. Our data for the ground-state transition are in reasonable agreement with the expectations of modern *ab initio* nuclear structure theory and support the spin-parity assignment of $3/2^-$ for the ground state. The current data are not consistent with the report of a very low-lying narrow state at $E_X = 600$ keV by Meister *et al*. Although the current data suggest that a resonance in ^{7}He at $E_X = 2.6$ MeV with $\Gamma \approx 2$ MeV may be populated in the (d, p) reaction that could correspond to a $1/2^-$ state, further study may help to clarify the nature of these very short-lived states in the continuum.

This work was supported by the U.S. Department of Energy, Office of Nuclear Physics under contract numbers DE-FG02-04R41320 (WMU), W-31-109-ENG-38 (ANL), DE-FG02-98ER4106 (NU), and the Faculty Research and Creative Activities Fund, Western Michigan University.

[1] R. H. Stokes and P. G. Young, Phys. Rev. Lett. **18**, 611 (1967).
[2] R. H. Stokes and P. G. Young, Phys. Rev. **178**, 2024 (1969).
[3] D. R. Tilley *et al*., Nucl. Phys. **A708**, 3 (2002).
[4] S. Cohen and D. Kurath, Nucl. Phys. **73**, 1 (1965); D. Kurath (private communication).
[5] A. A. Wolters, A. G. M. van Hees, and P. W. M. Glaudemans, Phys. Rev. C **42**, 2062 (1990).
[6] P. Navrátil and B. R. Barrett, Phys. Rev. C **57**, 3119 (1998).
[7] S. C. Pieper, R. B. Wiringa, and J. Carlson, Phys. Rev. C **70**, 054325 (2004).
[8] J. Wurzer and H. M. Hofmann, Phys. Rev. C **55**, 688 (1997).
[9] H. G. Bohlen *et al*., Phys. Rev. C **64**, 024312 (2001).
[10] A. Korsheninnikov *et al*., Phys. Rev. Lett. **82**, 3581 (1999).
[11] F. Skaza *et al*., Phys. Lett. **B619**, 82 (2005).
[12] M. Meister *et al*., Phys. Rev. Lett. **88**, 102501 (2002).
[13] D. Frekers, Nucl. Phys. **A731**, 76 (2004).
[14] G. V. Rogachev *et al*., Phys. Rev. Lett. **92**, 232502 (2004).
[15] P. Boutachkov *et al*., Phys. Rev. Lett. **95**, 132502 (2005).
[16] D. Halderson, Phys. Rev. C **70**, 041603(R) (2004).
[17] M. S. Golovkov *et al*., Phys. At. Nucl. **64**, 1244 (2001).
[18] B. Harss *et al*., Rev. Sci. Instrum. **71**, 380 (2000).
[19] A. H. Wuosmaa *et al*., Phys. Rev. Lett. **94**, 082502 (2005).
[20] M. H. Macfarlane and S. C. Pieper, Argonne National Laboratory Report ANL-76-11, Rev. 1 (1978).